Table 1 Comparison of the Simpson, Euler, and LGL spectral methods

Method	J_i	$\lvert J_i - J_{ana}\rvert$	N_p
Analytic solution	0.577678		
$N = 6$			
Simpson collocation	0.577668	0.00001	18
Euler differential inclusion	0.582800	0.005122	12
Pseudospectral (LGL)	0.577679	8.3251*e*-07	18
Spectral differential inclusion (LGL)	0.577679	1.177*e*-06	12
$N = 11$			
Simpson collocation	0.577678	0.00000	33
Euler differential inclusion	0.578935	0.001257	22
Pseudospectral (LGL)	0.577678	1.403*e*-07	33
Spectral differential inclusion (LGL)	0.577678	1.403*e*-07	22
$N = 21$			
Simpson collocation	0.577682	0.000004	63
Euler differential inclusion	0.577990	0.000312	42
Pseudospectral (LGL)	0.577678	1.403*e*-07	63
Spectral differential inclusion (LGL)	0.577678	1.403*e*-07	42

Table 2 Comparison of final states for the Simpson, Euler differential inclusion, and LGL methods

Method	$u(\tau_f)$	$x_1(\tau_f)$	$x_2(\tau_f)$
Analytic solution	1.347264	0.122881	0.474383
$N = 6$			
Simpson collocation	1.326334	0.122749	0.474333
Euler differential inclusion	N/A	0.131702	0.477656
Pseudospectral (LGL)	1.344669	0.122880	0.474382
Spectral differential inclusion (LGL)	N/A	0.123086	0.474459
$N = 11$			
Simpson collocation	1.342595	0.122815	0.474358
Euler differential inclusion	N/A	0.125050	0.475188
Pseudospectral (LGL)	1.347264	0.122881	0.474382
Spectral differential inclusion (LGL)	N/A	0.122876	0.474381
$N = 21$			
Simpson collocation	1.346748	0.122868	0.474377
Euler differential inclusion	N/A	0.123432	0.474587
Pseudospectral (LGL)	1.347264	0.122881	0.474382
Spectral differential inclusion (LGL)	N/A	0.122881	0.474383

Conclusions

The crux of the numerical optimal control problem is the implementation of the state dynamic equations. In direct collocation, the state equations are implemented as equality constraints, whereas in the differential inclusion approach they assume the form of both inequality and equality constraints. For the differential inclusion transformation to work, the value of the rate of change of state variables at the ith node should be expressible in terms of the discrete states. This hitherto limited the scope of the discretized differential inclusions to simple Euler integration rules. Consequently, the gains obtained in reducing the size of the problem in a differential inclusion transformation were lost due to the use of the less accurate Euler rule, which requires more nodes to maintain acceptable accuracy. The pseudospectral method presented here overcomes these drawbacks because the calculation of the state derivatives in this method allows for expressing the derivative at the ith node as a linear combination of values of the states at the discrete nodes. In this manner, the discretization of the derivative of the states is significantly different from the integration rules used in other collocation methods. The use of this highly accurate pseudospectral method in the discretization of the differential inclusion makes it quite competitive to direct collocation methods that employ high-order quadrature rules.

References

[1]Hargraves, C. R., and Paris, S. W., "Direct Trajectory Optimization Using Nonlinear Programming and Collocation," *Journal of Guidance, Control, and Dynamics*, Vol. 10, No. 4, 1987, pp. 338–342.

[2]Herman, A. L., and Conway, B. A., "Direct Optimization Using Collocation Based on High-Order Gauss–Lobatto Quadrature Rules," *Journal of Guidance, Control, and Dynamics*, Vol. 19, No. 3, 1996, pp. 592–599.

[3]Conway, B. A., and Larson, K. M., "Collocation vs Differential Inclusion in Direct Optimization," *Journal of Guidance, Control, and Dynamics*, Vol. 21, No. 5, 1998, pp. 780–785.

[4]Enright, P. J., and Conway, B. A., "Discrete Approximations to Optimal Trajectories Using Direct Transcription and Nonlinear Programming," *Journal of Guidance, Control, and Dynamics*, Vol. 15, No. 3, 1992, pp. 994–1002.

[5]Seywald, H., "Trajectory Optimization Based on Differential Inclusion," *Journal of Guidance, Control, and Dynamics*, Vol. 17, No. 3, 1994, pp. 480–487.

[6]Kumar, R. R., and Seywald, H., "Should Controls be Eliminated While Solving Optimal Control Problems via Direct Method?" *Journal of Guidance, Control, and Dynamics*, Vol. 19, No. 2, 1996, pp. 418–423.

[7]Canuto, C., Hussaini, M. Y., Quarteroni, A., and Zang, T. A., *Spectral Methods in Fluid Dynamics*, Springer-Verlag, New York, 1988.

[8]Gottlieb, D., Hussaini, M. Y., and Orszag, S. A., "Theory and Applications of Spectral Methods," *Spectral Methods for PDE's*, Society for Industrial and Applied Mathematics, Philadelphia, 1984, pp. 1–54.

[9]Elnagar, J., Kazemi, M. A., and Razzaghi, M., "The Pseudospectral Legendre Method for Discretizing Optimal Control Problems," *IEEE Transactions on Automatic Control*, Vol. 40, No. 10, 1995, pp. 1793–1796.

[10]Fahroo, F., and Ross, I. M., "Costate Estimation by a Legendre Pseudospectral Method," *Journal of Guidance, Control, and Dynamics* (to be published); also AIAA Paper 98-4222, 1998.

[11]Fahroo, F., and Ross, I. M., "Computational Optimal Control by Spectral Collocation with Differential Inclusion," *Proceedings of the 1999 Flight Mechanics Symposium*, NASA CP-1999-209235, 1999, pp. 185–200.

[12]Gill, P. E., Murray, W., Saunders, M. A., and Wright, M. A., "User's Guide to NPSOL 5.0: A Fortran Package for Nonlinear Programming," Standard Optimization Lab., TR 86-1, July 1998.

Integrated Design of Reconfigurable Fault-Tolerant Control Systems

Youmin Zhang* and Jin Jiang†

University of Western Ontario, London, Ontario N6A 5B9, Canada

Introduction

A FAULT-TOLERANT control system (FTCS) is a control system that possesses the ability to accommodate system component failures automatically. Such a control system is capable of maintaining overall closed-loop stability and performance in the event of failures. Research on the FTCS was started by the U.S. Air Force in an attempt to design self-repairing flight control systems[1] and by the aerospace industry to design restructurable (reconfigurable) flight control systems for commercial aircraft[2] in the mid-1980s. Typically, a reconfigurable FTCS consists of three parts: a reconfigurable controller, a fault detection and diagnosis (FDD) scheme, and a control law reconfiguration mechanism. The key issue is how to design those subsystems in an integrated way such that they can operate in harmony to recover the prefault system performance as much as possible.

The existing methods for reconfigurable controller design can be classified as linear quadratic regulator (LQR),[2] eigenstructure assignment (EA),[3] multiple model (MM),[4] adaptive control,[5] pseudoinverse,[6] and model following,[7] to name a few. However, most of these methods assume that a perfect FDD scheme is available and the postfault model of the system is known completely.

Received 11 January 2000; revision received 5 June 2000; accepted for publication 14 July 2000.

*Assistant Professor, Department of Electrical and Computer Engineering; ymzhang@julian.uwo.ca.

†Professor, Department of Electrical and Computer Engineering; jjiang@julian.uwo.ca.

In other words, the reconfigurable control laws are designed without any interaction with the FDD scheme. Generally speaking, a simple-minded combination of the two parts will not guarantee an operational FTCS. Therefore, it is highly desirable to develop new techniques that can integrate the FDD scheme and the reconfigurable control law in a coherent fashion without assuming knowledge of the postfault system model. Ideally, at each step of the controller reconfiguration, the FDD scheme should provide information on the postfault system in real time as precisely as possible, and the reconfigurable controller should be able to recover the performance of the prefault system to the maximum extent with consideration of the physical limitations of the system.

In this Note, an integrated approach to the design of online fault detection, diagnosis, and automatic reconfigurable control systems is proposed. The scheme includes a proportional-integral (PI) control structure to recover both the dynamic and steady-state performances of the prefault system and to reject unknown disturbances. A singular value decomposition (SVD)–based EA technique is developed to achieve online automatic redesign of the controller. Fault diagnosis and controller reconfiguration are carried out using online statistical hypothesis tests based on the information from a two-stage adaptive Kalman filter.[8] The approach has been applied to an aircraft example to deal with various type of actuator faults, for example, abrupt and incipient faults, partial and total faults, and single, multiple, and consecutive faults in the collective pitch control and the longitudinal cyclic pitch control channels.

Modeling of Actuator Faults as Loss in Control Effectiveness

Consider a fault-free system described by the following model:

$$x_{k+1} = Ax_k + Bu_k + w_k^x$$
$$y_k = H_r x_k, \qquad z_k = Hx_k + v_k \tag{1}$$

where $x_k \in \mathcal{R}^n$ is the system state and $u_k \in \mathcal{R}^l$ is the input. $y_k \in \mathcal{R}^p$ is the system output. H_r is a matrix that relates to the subset of outputs that track the reference inputs. $z_k \in \mathcal{R}^m$ represents the measurements used in the Kalman filter. w_k^x is a zero-mean white Gaussian process noise sequence with covariance Q_k^x representing the modeling errors. v_k is a zero-mean white Gaussian measurement noise sequence with covariance R_k. The initial state x_0 is a Gaussian vector with mean $\bar{x}_0$ and covariance $\bar{P}_0$.

To model actuator faults, control effectiveness factors have been introduced. The system-state equation in the presence of actuator faults can be written as

$$x_{k+1} = Ax_k + Bu_k + BU_k\gamma_k + w_k^x \tag{2}$$

where the control effectiveness vector $\gamma_k = [\gamma_k^1 \ \gamma_k^2 \ \cdots \ \gamma_k^l]^T$ represents the actuator status. $\gamma_k^i = 0$ indicates a healthy actuator, $\gamma_k^i = 1$ corresponds to a total failure of the ith actuator, and $0 < \gamma_k^i < 1$ represents a partial loss in the control effectiveness; $U_k = \text{diag}[-u_k^1 \ -u_k^2 \ \cdots \ -u_k^l]$.

The goal of the FDD scheme is to determine the location and the extent of the loss in the control effectiveness, γ_k, so that the reconfigurable control law can be synthesized accordingly. In the absence of knowledge of the true status of the control effectiveness factors, they can be modeled as a random bias vector:

$$\gamma_{k+1} = \gamma_k + w_k^\gamma \qquad \begin{cases} \gamma_k = 0, & k < k_F \quad \text{fault-free} \\ \gamma_k \neq 0, & k \geq k_F \quad \text{fault} \end{cases} \tag{3}$$

where k_F denotes the unknown time instance at which the fault has occurred, and w_k^γ accounts for the random characteristics in γ_k and the modeling uncertainty.

Consequently, the combined state and control effectiveness model has the following form:

$$x_{k+1} = Ax_k + Bu_k + BU_k\gamma_k + w_k^x$$
$$\gamma_{k+1} = \gamma_k + w_k^\gamma, \qquad z_k = Hx_k + v_k \tag{4}$$

where w_k^γ is a zero-mean white Gaussian sequence with covariance Q_k^γ.

Given the previous fault model, the objective of the proposed scheme is to 1) estimate the system state and the control effectiveness simultaneously, 2) detect and diagnose the fault in terms of the loss of the control effectiveness, and 3) recover the system performance to the maximum extent via online controller reconfiguration.

Reconfigurable Control with PI Actions

To achieve the command tracking in the presence of noise, disturbance, and uncertainty, PI control strategy has been widely used in practice. In this Note, PI control action is to be incorporated in the design of the reconfigurable FTCS to achieve satisfactory recovery of both transient and steady-state performance and to reject unknown disturbances. Figure 1 illustrates the overall configuration of this scheme.

To incorporate the integral action into the controller design, we can consider an integrator as an augmented state. In the discrete domain, the state-space representation of multiple integrators can be described as

$$e_{k+1}^I = e_k^I + Te_k \tag{5}$$

where e_k is the tracking error defined as $e_k = r_k - y_k$. T is the sample period.

The feedback control is required to make the output y_k track the command input r_k so that at the steady-state

$$\lim_{k\to\infty} y_k = r_k \tag{6}$$

where $r_k \in \mathcal{R}^p$ consists of piecewise constant-command inputs.

To achieve this objective, an augmented state vector is defined $X_k^T = [x_k^T \ e_k^{I^T}]$, and the augmented closed-loop system can be represented by

$$X_{k+1} = \left(\bar{A} + \bar{B}_k^f K\right)X_k + Fr_k + Gw_k^x \tag{7}$$

where

$$\bar{A} = \begin{pmatrix} A & 0 \\ -TH_r & I \end{pmatrix}, \qquad \bar{B}_k^f = \begin{pmatrix} B_k^f \\ 0 \end{pmatrix}$$
$$F = \begin{pmatrix} 0 \\ TI \end{pmatrix}, \qquad G = \begin{pmatrix} I \\ 0 \end{pmatrix} \tag{8}$$

and the closed-loop control signal is described as

$$u_k = KX_k = [K_P \quad K_I]\begin{pmatrix} x_k \\ e_k^I \end{pmatrix} \tag{9}$$

where K_P and K_I are the proportional and integral gains of the controller, respectively.

For the augmented system, a control law of the form in Eq. (9) can be synthesized such that the output of the closed-loop system tracks a constant command input. Since the stability and dynamic

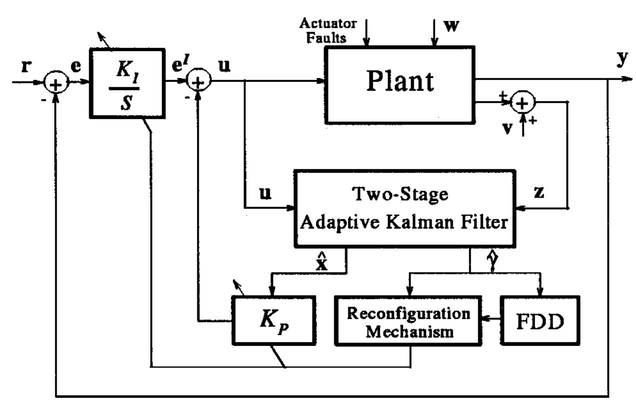

Fig. 1 Integrated FDD and reconfigurable control structure.

performance of a system is governed not only by its eigenvalues, but also by the associated eigenvectors. To ensure the stability and to recover the performance after a fault, the eigenstructure of the reconfigured system should be assigned as close to that of the prefault system as possible if sufficient actuator redundancy exists (in terms of actuator power rating).

An SVD-based eigenstructure assignment technique has been developed for calculating the reconfigurable controller gains. Detailed calculation of K_P and K_I can be found in Ref. 9.

Integration of the FDD and the Reconfiguration Mechanism

Estimation of States and Control Effectiveness Factors

To achieve online controller reconfiguration, it is necessary to obtain the state and to determine the control input matrix B_k^f in the event of actuator failure. This is a combined state and parameter estimation problem. The control input matrix can be calculated by $B_k^f = B(I - \Gamma_k)$, $\Gamma_k = \mathrm{diag}[\gamma_k^1 \ \ \gamma_k^2 \ \ \cdots \ \ \gamma_k^l]$. To estimate both $\boldsymbol{x}_k$ and γ_k effectively, a two-stage adaptive Kalman filter[8] has been used.

With the integrated FDD and the reconfigurable control structure illustrated in Fig. 1, it is important to note that the input signal to the Kalman filter is a closed-loop signal that can be obtained at the controller output:

$$\boldsymbol{u}_k = K_P \hat{\boldsymbol{x}}_{k|k} + K_I \boldsymbol{e}_k^I, \qquad \boldsymbol{e}_k^I = \boldsymbol{e}_{k-1}^I + T(\boldsymbol{r}_k - H_r \hat{\boldsymbol{x}}_{k|k}) \quad (10)$$

FDD Scheme

For online reconfiguration purposes, an FDD scheme is needed to provide information for fault time, location, and type as soon as the failure occurs. The magnitude of the actuator faults is further obtained from the estimates of control effectiveness factors. To provide fast and reliable FDD, the statistical hypothesis test[10] has been adopted.

Reconfiguration Mechanism

After the fault has been detected, one still has to decide the best starting time to activate the reconfiguration process. To avoid excessive fault-induced transients in the system and recover the prefault system performance, should the reconfiguration process start right after the fault is declared or should one wait for some time until a more accurate fault parameter estimate becomes available? Because it is important to design reconfigurable control law based on the converged control effectiveness factor estimates, it is found that to achieve good reconfiguration performance, the activation of the reconfiguration process should take place only when the errors in consecutive control effectiveness factor estimates satisfy the following smooth condition:

$$\left|\hat{\gamma}_k^i - \hat{\gamma}_{k-1}^i\right| \le \delta_i, \qquad i = 1, \ldots, l \quad (11)$$

The threshold δ_i is a design parameter.

Example and Performance Evaluation

In this section, the effectiveness of the proposed scheme will be demonstrated through an example of a linearized longitudinal vertical takeoff and landing (VTOL) aircraft model.[11]

Simulation Example

The discretized model of the VTOL aircraft with the sampling period $T = 0.1$ s has been used for simulation, where $\boldsymbol{x} = [u \ \ v \ \ q \ \ \theta]^T$, $\boldsymbol{u} = [\mu_c \ \ \mu_l]^T$. The states of the system are horizontal velocity u, vertical velocity v, pitch rate q, and pitch angle θ. The two control inputs are collective pitch control μ_c, and longitudinal cyclic pitch control μ_l. To track the horizontal velocity and vertical velocity, the H_r and H matrices are given as

$$H_r = H = \begin{pmatrix} 0 & 1 & 0 & 0 \\ 1 & 0 & 0 & 0 \end{pmatrix}$$

Parameters used are as follows: $Q^x = \mathrm{diag}\{0.01^2, \ 0.01^2, \ 0.01^2, \ 0.01^2\}$, $Q^\gamma = \mathrm{diag}\{0.001^2, \ 0.001^2\}$, $R = \mathrm{diag}\{0.1^2, \ 0.1^2\}$, $\boldsymbol{x}_0 = [20 \ \ 5 \ \ 8 \ \ 1]^T$, and $\gamma_0 = [0 \ \ 0]^T$. Initial parameters of the Kalman filter are $\tilde{\boldsymbol{x}}_0 = \boldsymbol{x}_0$, $\hat{\gamma}_0 = \gamma_0$, $\tilde{P}_0 = 10I$, $P_0^\gamma = 10I$, $Q_k^x = Q^x$, $Q_k^\gamma = Q^\gamma$, and $R_k = R$. The controller for the prefault system is designed using an LQR technique, the state and the control weighting matrices are chosen to be $Q_{\mathrm{LQR}} = \mathrm{diag}\{1, 1, 1, 1\}$ and $R_{\mathrm{LQR}} = \mathrm{diag}\{1, 1\}$, respectively.

Measures for Performance Evaluation

Because it is desirable to have short transient response and small steady-state error, the following normalized measures are used in the performance evaluation:

$$e_k = \frac{\left\| \boldsymbol{y}_k^{\mathrm{normal}} - \boldsymbol{y}_k^{\mathrm{reconfigured}} \right\|_2}{\left\| \boldsymbol{y}_k^{\mathrm{normal}} \right\|_2} \quad (12)$$

where $\boldsymbol{y}_k^{\mathrm{normal}}$ denotes the output of the fault-free system and $\boldsymbol{y}_k^{\mathrm{reconfigured}}$ represents the output of the reconfigured system.

In addition, the average and the maximum values of e_k, $\forall k \in \{1, N\}$ are also used:

$$\bar{e} = \frac{1}{N}\sum_{k=1}^{N} e_k, \qquad e_{\max} = \max\{e_k\} \qquad \forall k \in \{1, N\} \quad (13)$$

where N is the total number of the data points (200) used in the simulation.

Fault Scenarios and Reference Inputs

To simulate different situations of actuator faults, three arbitrarily designed fault scenarios were selected: a loss of the control effectiveness in a single actuator (S1), simultaneous loss of the control effectiveness in both actuators (S2), and an abrupt loss followed by a gradual loss in one actuator, then followed by an abrupt loss in the second actuator (S3).

To demonstrate the effectiveness of the proposed scheme for tracking different reference inputs even in the presence of actuator faults, two types of inputs, constant and arbitrarily varying, have been used.

System Performance in Different Cases

The vertical velocity of the reconfigured system under the condition of a constant reference input in the S2 is shown in Fig. 2. In this case, simultaneous partial faults have been considered where a 95% loss of the control effectiveness in the first actuator and a 75% loss of the control effectiveness in the second actuator occurred at $t_F = 5$ s. For comparison purposes, the response under the normal condition and the one without the controller reconfiguration are also demonstrated. To evaluate the performance of the designed reconfigurable control system under the actuator saturation, the response with a limit of $|\boldsymbol{u}|_{\max} = 5$ for both closed-loop control signals is also illustrated.

The proposed approach has recovered both the dynamic and the steady-state performance of the prefault system with a short

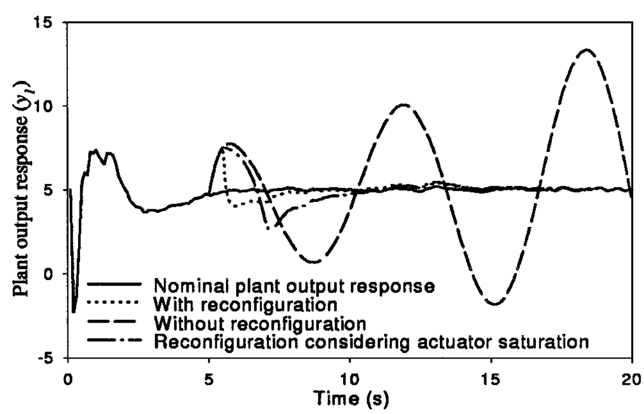

Fig. 2 Output with constant reference inputs.

transient. However, the system will become unstable if left without reconfiguration. It is interesting to note that before the reconfiguration process is activated at $t = 5.4$ s, the output of the closed-loop system tends to diverge. This means that the system has to be reconfigured as soon as possible to prevent saturation and disintegration. After the reconfigurable control law has been initiated, the stability and performance of the system are recovered. The reconfigured system can track the reference input $\boldsymbol{r}_k = [5 \;\; 5]^T$ even in the presence of the fault. Furthermore, even if the actuator saturation has occurred under the given control signal limits, the scheme can still maintain excellent overall performance.

Table 1 illustrates the corresponding detection time (t_D) and reconfiguration time (t_R). The average and maximum values of the performance index e_k with and without reconfiguration are further given in Table 2 for all three test scenarios. Based on the results in Table 2, for different type of actuator faults, excellent results have been achieved via the developed integrated FDD and the reconfigurable control scheme.

Table 1 Fault detection and reconfiguration time

Faults	t_F	t_D	t_R
Actuator 1	5.0	5.3	5.4
Actuator 2	5.0	5.3	5.5

Table 2 Performance with and without reconfiguration

Performance	Index	S1	S2	S3
With reconfiguration	$\bar{e}$	0.0188	0.0796	0.0246
	$e_{\max}$	0.4722	0.5042	0.1395
Without reconfiguration	$\bar{e}$	0.0875	0.4607	0.0339
	$e_{\max}$	0.4834	1.1753	0.1402

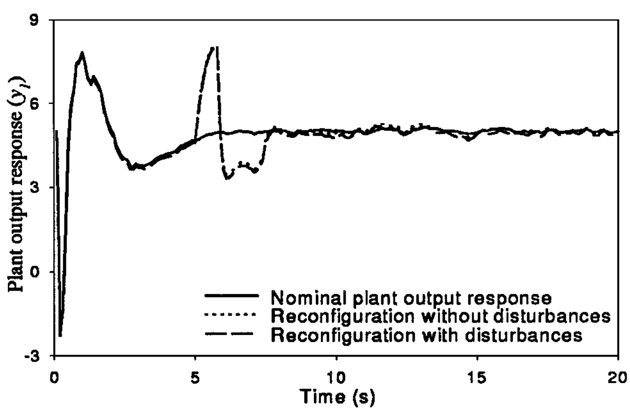

Fig. 3 Output in the presence of disturbances.

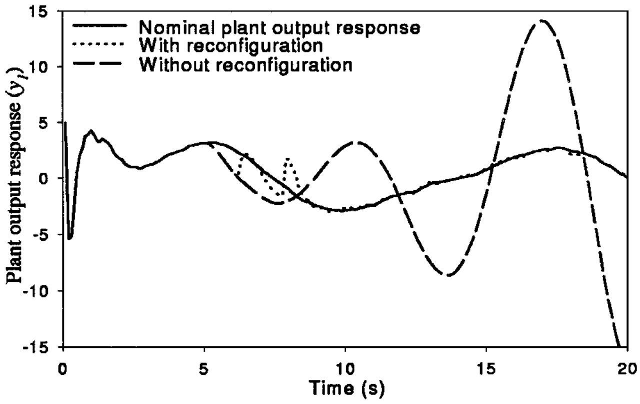

Fig. 4 Output with time-varying inputs.

To evaluate the performance of the proposed scheme in the presence of both unknown faults and disturbances, a constant disturbance of magnitude 0.1 (about 10% compared to the maximum fault magnitude) and a time-varying disturbance (turbulence) have been added to each of the measurement variables. The vertical velocity of the reconfigured system in the presence and absence of such disturbances for S2 is shown in Fig. 3. It can be seen that even in the presence of constant and time-varying disturbances, the proposed scheme can still obtain an excellent performance.

To show that the proposed scheme has the ability to effectively recover the performance of the prefault system even with general reference input, the results for the S2 under the arbitrarily varying reference inputs are illustrated in Fig. 4. It can be observed that the satisfactory reconfiguration performance has also been achieved in this case. Without the reconfiguration, however, the system becomes unstable.

Conclusions

An integrated FDD and reconfigurable control system design approach has been investigated in this Note. The proposed scheme is based on a two-stage adaptive Kalman filter for state and fault parameter estimation, the statistical decisions for fault detection, diagnosis and activation of the controller reconfiguration, and the reconfigurable control law design based on the EA technique. Design of these subsystems is carried out automatically online. Effective recovery of the performance in the presence of reference inputs and the unknown disturbances has been achieved using the proportional-integral control structure. The proposed approach is capable of dealing with different types of actuator faults and different types of reference inputs, disturbances, and random noises. The design technique has been applied to an aircraft control problem. Simulation results have demonstrated the effectiveness of the approach.

References

[1]Chandler, P. R., "Self-Repairing Flight Control System Reliability and Maintainability Program Executive Overview," *Proceedings of the IEEE National Aerospace and Electronics Conference*, Inst. of Electrical and Electronics Engineers, New York, 1984, pp. 586–590.

[2]Looze, D. P., Weiss, J. L., Eterno, J. S., and Barrett, N. M., "An Automatic Redesign Approach for Restructurable Control Systems," *IEEE Control Systems Magazine*, Vol. 5, May 1985, pp. 16–22.

[3]Jiang, J., "Design of Reconfigurable Control Systems Using Eigenstructure Assignment," *International Journal of Control*, Vol. 59, No. 2, 1994, pp. 395–410.

[4]Maybeck, P. S., and Stevens, R. D., "Reconfigurable Flight Control via Multiple Model Adaptive Control Methods," *IEEE Transactions on Aerospace and Electronic Systems*, Vol. 27, No. 3, 1991, pp. 470–479.

[5]Bodson, M., and Groszkiewicz, J., "Multivariable Adaptive Algorithms for Reconfigurable Flight Control," *IEEE Transactions on Control System Technology*, Vol. 5, No. 2, 1997, pp. 217–229.

[6]Caglayan, A. K., Allen, S. M., and Wehmuller, K., "Evaluation of a Second Generation Reconfiguration Strategy for Aircraft Flight Control Systems Subjected to Actuator Failure/Surface Damage," *Proceedings of the IEEE National Aerospace and Electronics Conference*, Inst. of Electrical and Electronics Engineers, New York, 1988, pp. 520–529.

[7]Huang, C. Y., and Stengel, R. F., "Restructurable Control Using Proportional-Integral Implicit Model Following," *Journal of Guidance, Control, and Dynamics*, Vol. 13, No. 2, 1990, pp. 303–309.

[8]Wu, N. E., Zhang, Y. M., and Zhou, K., "Control Effectiveness Estimation Using an Adaptive Kalman Estimator," *Proceedings of the IEEE International Symposium on Intelligent Control*, Inst. of Electrical and Electronics Engineers, New York, 1998, pp. 181–186.

[9]Zhang, Y. M., and Jiang, J., "Design of Proportional-Integral Reconfigurable Control Systems via Eigenstructure Assignment," *Proceedings of the American Control Conference*, American Automatic Control Council, Chicago, 2000, pp. 3732–3736.

[10]Zhang, Y. M., and Jiang, J., "Design of Integrated Fault Detection, Diagnosis and Reconfigurable Control Systems," *Proceedings of the 38th IEEE Conference on Decision and Control*, Inst. of Electrical and Electronics Engineers, New York, 1999, pp. 3587–3592.

[11]Narendra, K. S., and Tripathi, S. S., "Identification and Optimization of Aircraft Dynamics," *Journal of Aircraft*, Vol. 10, No. 4, 1973, pp. 193–199.